

Synthesis of Cellulose Aerogels from Coir Fibers via a NaOH/Urea Method for Methylene-blue Adsorption

Ngoc Tram Thi Nguyen^a, Nghiep Quoc Pham^b, Cong Minh Pham^b, Chinh Nguyen Dinh^b, Anh Khoi Tran^a, Minh Hieu Nguyen^a, Phung Thi Kim Le^a, Kien Anh Le^{b,*}, V. Cuong Tran^b

^a Ho Chi Minh city University of Technology, 268 Ly Thuong Kiet street, district 10, Ho Chi Minh City, Vietnam.

^b Institute for Tropical Technology and Environmental Protection, 57A Truong Quoc Dung street, ward 10, Phu Nhuan district, Ho Chi Minh city, Vietnam.

leanhkien@hcmut.edu.vn

Coir (i.e., coconut fiber) is one of the popular agricultural waste products, especially in Vietnam, mostly discarded when copra and coconut water are taken, causing environmental pollution and waste of potential biomass. Various research has been done to reuse this resource as advanced materials. In this study, the NaOH-urea-H₂O₂ combination was utilized to make cellulose aerogel from coir fibers for the first time. Cellulose aerogel was synthesized by the sol-gel method combined with the freeze-drying technique. The properties of cellulose aerogel were determined, such as density, porosity, surface morphology analysis by FTIR, SEM, and thermal stability evaluation by TGA analysis. They exhibit low density (0.0099 - 0.0158 g/cm³), high porosity (98.96 - 99.35 vol%), and the methyl blue adsorption experiment shows cellulose aerogel's ability to treat color in water is significant.

1. Introduction

Aerogels have been widely used in different fields due to their excellent properties (Yang et al., 2019). It is known to be a porous solid material with a high specific density and surface area (Manzocco and Mikkonen, 2021). In searching for green materials for aerogel fabrication, biopolymers have been thought to be the next promising precursors (Antonyuk et al., 2015). In 2017, Goimil and colleagues studied the mechanical toughness and biodegradability of bio-aerogels. The results showed the most remarkable advantages in the research (Goimil et al., 2017). Kargazadeh et al. (2018) synthesized bio-aerogel from biofilm-forming agents such as polysaccharides, while Ahmadi et al. (2016) used proteins. Yang et al. (2017) successfully synthesized polysaccharides aerogels from agar, nitrocellulose or cellulose with superior properties. The unique biodegradability, biocompatibility, sustainability, and renewability of polysaccharide aerogels at comparatively low cost make them ideal for medical, pharmaceutical and food applications (Sarno, 2019).

The development of green technologies for cellulose processing is always content of discussion in the field of sustainable chemistry. During the last two decades, some potent non-derivatizing organic solvents for cellulose have been created and used to prepare regenerated cellulose films and fibers, such as N-methyl morpholine-N-oxide (NMMO) (Fink et al., 2001), and the ionic liquids (Swatloski et al., 2002). Eco-friendly, simple and economic processes are realized with a solvent system based on NaOH and cellulose.

Compared with different types of biomass such as cotton stalks, paper waste, and cotton waste, the lignin content in coir fiber is much higher, which prevents the NaOH-urea process from being applied directly. The aerogel produced will become hard, brittle, and difficult to squeeze if the lignin content is too high (Fauziyah et al., 2019). Large pores in the aerogel network are formed due to the existence of lignin in the endogenous state (in coconut fiber). For cellulose aerogels, the increased endogenous lignin restricts the dissociation of cellulose and hemicellulose, causes a membrane-like structure, and weakens the interphase between cellulose or hemicellulose chains in the aerogel network, thus leading to larger pores and reduced mechanical properties (Cai and Zhang, 2005). A study on the effect of coir components on dye adsorption was performed by Mishra.

The gradual removal of lignin and hemicelluloses changes the composition and functional groups of crude coir. The dye adsorption capacity of the material increased as the amount of lignin removed increased. Increasing the cellulose content due to the removal of hemicelluloses improved the primary dye uptake due to structural swelling and supported a higher degree of reactive dye uptake. Fauziyah et al. (2019) has synthesized cellulose aerogels for various applications such as oil, water, and dye adsorption. Fauziyah et al. (2020) synthesized hydrophobic cellulose aerogel used to separate contaminated oil. However, the effect of fibers concentration on the properties and adsorption capacity of cellulose aerogels has not been reported.

In this study, cellulose aerogels are synthesized from coir fiber by sol-gel process combined with freeze-drying. Compared with previous studies, in the pretreatment of coconut fibers, an additional treatment step with H₂O₂-NaOH solution will be added to remove the most significant amount of lignin. Evaluation of methylene blue adsorption capacity of cellulose aerogels with different fiber concentrations was conducted by ultraviolet-visible spectroscopy.

2. Material and Methods

2.1 Materials

Coir fibers used were obtained from the husk of coconut in Vietnam. Hydrogen peroxide (H₂O₂), sodium hydroxide (NaOH), urea (CON₂H₄) and ethanol (C₂H₅OH) were of reagent grade and were used as received without further purification. Deionized water was used for synthesis and treatment processes.

2.2 Fabrication of the cellulose aerogels

Coir fibers were alkaline treated for the first time with 6 % NaOH solution with a solid-liquid ratio of 1:20 % w/v to remove part of the lignin from the coir fibers. The mixture was reacted at 90 °C for 2 h and repeated three times. The mixture was filtered and washed with distilled water to pH 7, and the residue was recovered after filtering. The second alkalization was performed, using 4 % NaOH solution according to the ratio (1 g coconut fibers / 20 g NaOH solution), stirred at 90 °C for 4 h. The obtained pulp was washed with demineralized water to remove the sodium–lignin by-product. The coir fiber pulp was dried for weighing to determine the weight for the next bleaching experiment. The coir fiber pulp was then bleached with a mixture of H₂O₂ and NaOH (a ratio of 1:1 % w/w) with the same concentration of 10 wt%; the solid-liquid ratio was kept at 1:20 % w/v. The bleaching reaction was carried out at 80 °C for 2 h. The mixture was filtered and washed to pH 7 with water and dried to obtain bleached coir fiber pulp. To prepare the cellulose aerogel precursor, the pulp could be used as material. Treated coir fibers are added to 25 mL of mixed NaOH/urea solution (7:12 wt%), which has been cooled to -10 °C. The bleached coir fibers pulp was dissolved into the solution using a magnetic stirrer for 30 min. The solution was then frozen for 24 h to form a gel system. After being frozen, the gel system was thawed at room temperature for 10 min, and ethanol added; the water inside the hydrogel was replaced with ethanol for 24 h. The gel was washed with water several times until pH 7. The sample was frozen at -10 °C for 12 h. Drying of the sample was carried out for 48 h to form cellulose aerogel.

2.3 Characterization

The bulk density of the aerogels ($\rho_{\text{cellulose aerogels}}$) was calculated using the Eq(1):

$$\rho_{\text{cellulose aerogels}} = \frac{m_{\text{cellulose aerogels}}}{V_{\text{cellulose aerogels}}} \quad (1)$$

where m (g) is mass of cellulose aerogel, V (cm³) is the volume of cellulose aerogels.

The porosity of the cellulose aerogel was calculated in the Eq(2):

$$\text{Porosity, } P = 1 - \frac{\rho_{\text{cellulose aerogels}}}{\rho_{\text{cellulose}}} \quad (2)$$

Where $\rho_{\text{cellulose}}$ (1.528 g/cm³) is the density of bulk cellulose (Wan et al., 2015).

Crosslinking of the cellulose aerogels by NaOH–urea was observed using Fourier transform infrared spectroscopy (FTIR; PerkinElmer Spectrum) over the wavenumber range of 400–4,000 cm⁻¹.

2.4 Adsorption experiments

Methylene blue (MB) (50 ppm) solution was prepared before testing. Adsorption experiments was conducted with 5 samples of synthesized materials of different fibers concentrations (2, 3, 4, 5, 6 wt%). Each material sample was weighed approximately 0.05 g into 25 mL MB. After 30, 60, 90, 120, 150 min, the solution was filtered and was measured the absorbance by UV-Vis machine (UV-VIS; Lovibond XD 7000) at 640 nm to determine the remaining MB concentration. The adsorption capacity of the samples can be calculated from Eq(3):

$$(\rho_L - \rho_G) \cdot g \cdot V_B = \pi a^2 \frac{\rho_L U_0^2}{2} \cdot f \quad (3)$$

where q_e is the adsorption capacity at equilibrium, C_0 and C_e are the initial and equilibrium MB concentration, V and m are the volume of the MB solution and mass of the adsorbent.

3. Results and Discussion

3.1 Morphology and structure of the cellulose aerogels

Figure 1 shows the dependence of density and porosity of cellulose aerogels on fiber concentrations. The cellulose aerogels obtained have extremely low densities (0.0099-0.0158 g/cm³) and high porosities (98.96-99.35 vol%), which indicates the light weight and the porous structures of the cellulose aerogels. The cellulose aerogels have denser network and less porosity with increasing cellulose concentration. Therefore, it can be larger cellulose concentrations in the initial solution can take up more space in the cellulose aerogels. More cross-linking bonding fewer can cause more packed and less air pockets in the cellulose aerogel network, as shown in Figure 3.

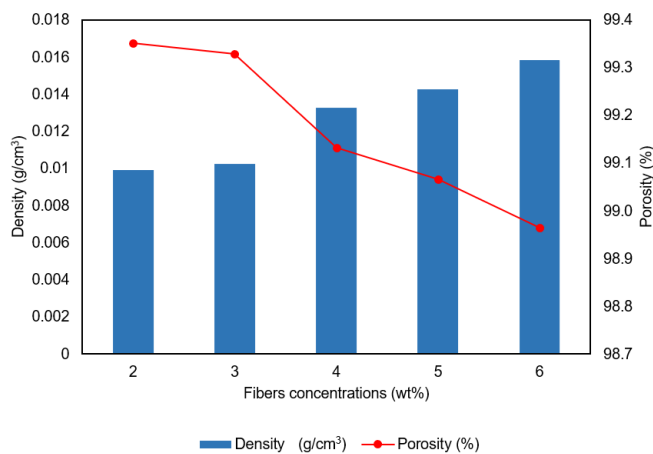


Figure 1: Densities and porosities of the cellulose aerogels with the different cellulose concentrations

The FTIR spectra of the different samples are presented in Figure 2. For all samples, there were four main bands corresponding to cellulose.

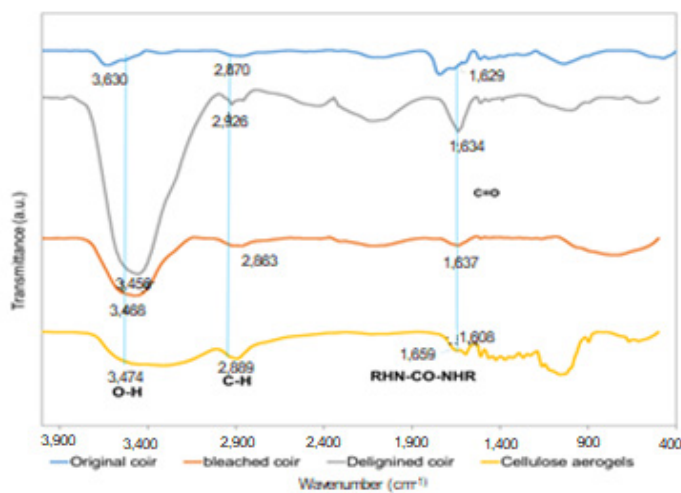


Figure 2: The FTIR spectra of different samples: (a) original coir; (b) delignified coir; (c) bleached coir; and (d) coir aerogel

The band at $3,474\text{ cm}^{-1}$ can be attributed to intramolecular hydrogen bonding (O–H stretching) of cellulose, and the band at $2,926\text{ cm}^{-1}$ corresponds to C–H stretching in $-\text{CH}$ and $-\text{CH}_2$ of cellulose compounds (Kathirselvam et al., 2019). The bands at $1,637\text{ cm}^{-1}$ are attributed to carbonyl (C=O) stretching of acetyl groups in hemicellulose or α -keto carboxylic acid in lignin. The bands in the samples after treatment of NaOH-urea and in the aerogel were shifted slightly to the right. These results indicate that the alkali hydrate, urea hydrate, and free water destroyed the intra- and intermolecular hydrogen bonding of cellulose and physically caused cellulose swelling in the solution (Cai and Zhang, 2005). These phenomena implied that NaOH-urea treatment by chemical changed the structure of cellulose from cellulose I to cellulose II (Oh et al., 2005). A new band at $1,660\text{ cm}^{-1}$ appeared in the spectra of solid samples after the addition of NaOH and urea. The band can be attributed to the functional group of urea ($\text{RHN}-\text{CO}-\text{NHR}$) (Baldanza et al., 2018). This urea band also appears in the spectrum of the cellulose aerogel but is slightly shifted to the right, which the dissolution of urea may cause with cellulose. The addition of NaOH-urea played an important role in the formation of the aerogel structure, and the NaOH-urea changed the structure of cellulose in physic and chemical.

Figure 3 shows the SEM images of the cellulose aerogels. The highly porous structure aerogel consists of an interconnected network of homogeneous cellulose fibers, as depicted in Figure 3a. The structures consist of a three-dimensional network of macrospore-forming filaments, each $20\text{--}200\text{ }\mu\text{m}$ in diameter. This lattice structure, which is formed by cross-linking of cellulose as mentioned above, confirms that NaOH-urea has good solubility. Figures 3b and 3c show the longitudinal and cross-sectional images of the cellulose fibers. The fibers themselves have a cylindrical-like structure with a diameter of $40\text{--}70\text{ }\mu\text{m}$ and are successfully self-assembled via hydrogen bonding to form a network of open pores. The fibers also have pores with a diameter of $2\text{--}4\text{ }\mu\text{m}$, as depicted in Figure 3c. The internal fiber pores also contribute to the increased porosity of the aerogel.

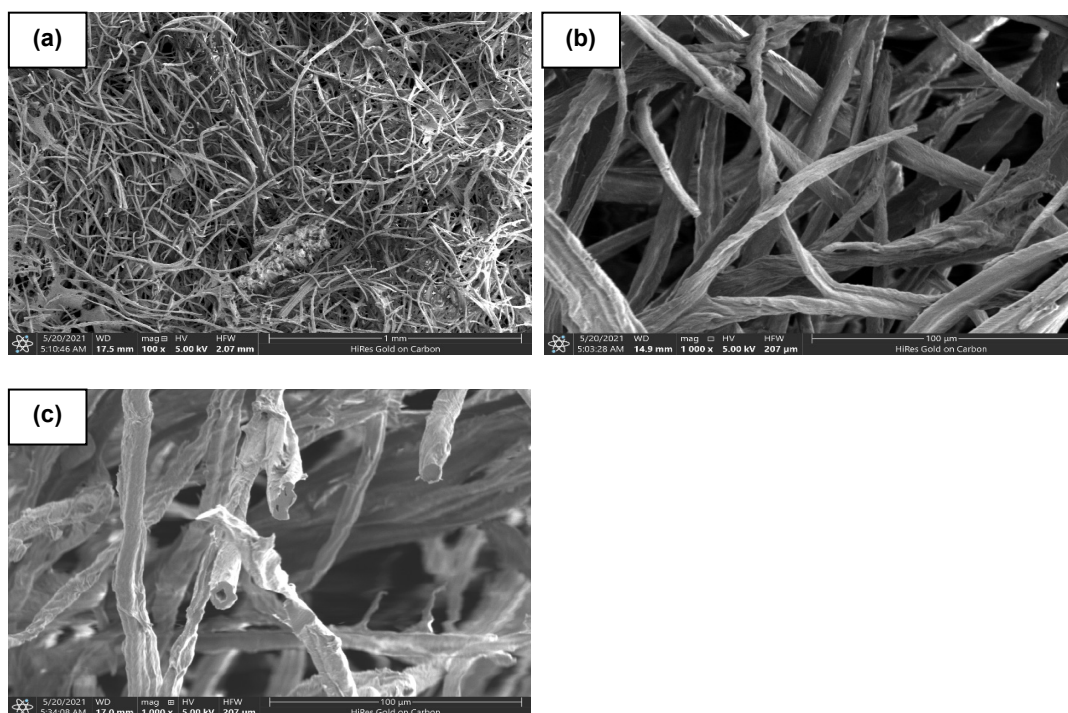


Figure 3: SEM images of coir aerogels: (a) an interconnected network of homogeneous cellulose fibers, (b) the longitudinal and (c) cross-sectional images of the cellulose fibers

3.2 Thermal stability of the cellulose aerogels

The thermal behaviour of cellulose aerogel with different fiber concentrations was evaluated at $25 - 1,000\text{ }^{\circ}\text{C}$ under nitrogen. It can be observed that for all samples, a small weight loss was detected between $25 - 150\text{ }^{\circ}\text{C}$ due to the evaporation of water (Figure 4). The second weight loss in the temperature range $250 - 350\text{ }^{\circ}\text{C}$ represents the simultaneous decomposition of cellulose and lignin compounds. The third weight loss was again the breakdown of cellulose and lignin, which occurred from a temperature of $350\text{ }^{\circ}\text{C}$ for different cellulose aerogel samples. It is obvious that the decomposition temperature range is higher when the lignin content is higher. The weight loss curve further slowed down after the third weight loss phase, indicating that the aerogel was carbonized at high temperatures. Cellulose aerogel 3 wt% is carbonized with a coal yield of 15.8% , and

aerogel cellulose 4 wt% and 6 wt% are carbonized with an average coal yield of 19 %. The decomposition temperatures of cellulose aerogels were higher than those of materials prepared from coconut shells (200-400 °C) (Wan et al., 2015) and shredded paper (230-330 °C) (Nguyen et al., 2014), possibly due to the presence of residual lignin in the pulp.

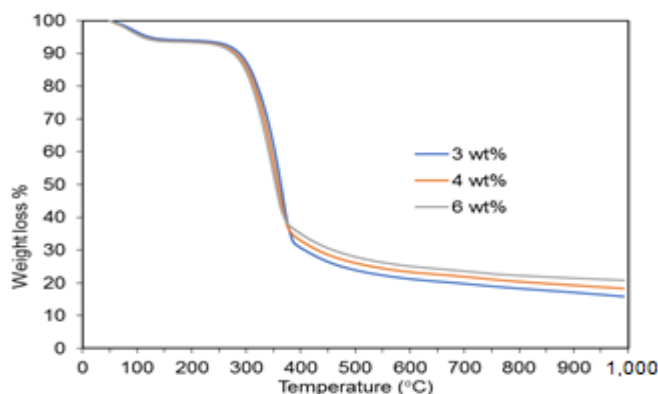


Figure 4: Thermogravimetric analysis (TGA) results for coir fiber and cellulose aerogels

3.3 Evaluate the adsorption capacity of cellulose aerogels

Figure 5 shows that methylene blue (MB) adsorption by cellulose aerogel is similar to different fiber concentrations. During the initial 30 min, the adsorption capacity increased rapidly. The MB adsorption capacity is inversely proportional to the fiber concentration in the adsorbent sample. At 15 min, the 2 wt% sample had an adsorption capacity of 17.68 mg/g and the 6 wt% sample was 14.14 mg/g. In 2020, Beh reports cellulose aerogel derived from sago pith waste was efficient in MB removal with a maximum MB adsorption of 222.2 mg/g at 20 °C (Beh et al., 2020). While cellulose aerogels from polyvinyl alcohol and M-K10 fibers have a low density of 0.0193 g/cm³ and methylene blue (20 ppm) adsorption capacity is 2.28 mg/g (Luo et al., 2021). This proves that samples with low fibers concentration will have high porosity and better MB adsorption. Over time, the adsorption rate gradually decreased. More active sites exist on cellulose aerogels in the initial state of adsorption, and the higher MB concentration results in higher adsorption rates. As the adsorption time increased, the adsorption sites of cellulose aerogel were occupied by MB, the MB concentration decreased, and the adsorption pulse decreased, so the adsorption rate decreased.

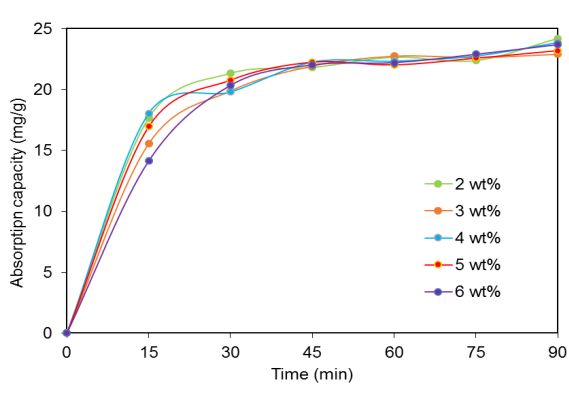


Figure 5: Effect of fibres concentration on MB adsorption capacity

4. Conclusion

In this study, cellulose aerogel was synthesized from coir fiber by sol-gel process combined with freeze-drying. Evaluation of the effect of coir fiber concentration on physicochemical properties of cellulose aerogel and methyl green adsorption capacity was performed. The aerogel morphology depends much on the coir fiber content. The thermal and mechanical properties can be enhanced by increasing the fibres content in the aerogel. The results show that cellulose aerogel from coir fiber has effective applicability for colour treatment in water.

Acknowledgements

The research is funded by Ho Chi Minh City Foundation for Science and Technology Development, under grant number 109/2020/HĐ-QPTKHCN.

References

- Ahmadi M., Madadlou A., Saboury A. A., 2016, Whey protein aerogel as blended with cellulose crystalline particles or loaded with fish oil, *Food Chemistry*, 196, 1016-1022.
- Antonyuk S., Heinrich S., Gurikov P., Raman S., Smirnova I. 2015, Influence of coating and wetting on the mechanical behaviour of highly porous cylindrical aerogel particles, *Powder Technology*, 285, 34-43.
- Baldanza V. A. R., Souza Jr F. G., Filho S. T., Franco H. A., Oliveira G. E., Caetano R. M. J., Hernandez J. A. R., Ferreira Leite S. G., Furtado Sousa A. M., Nazareth Silva A. L., 2018, Controlled-release fertilizer based on poly(butylene succinate)/urea/clay and its effect on lettuce growth, *Journal of Applied Polymer Science*, 135(47), 46858.
- Beh J. H., Lim T. H., Lew J. H., Lai J. C., 2020, Cellulose nanofibril-based aerogel derived from sago pith waste and its application on methylene blue removal, *International Journal of Biological Macromolecules*, 160, 836-845.
- Cai J., Zhang L., 2005, Rapid dissolution of cellulose in LiOH/urea and NaOH/urea aqueous solutions, *Macromolecular Bioscience*, 5(6), 539-548.
- Fink H. P., Weigel P., Purz H. J., Ganster J., 2001, Structure formation of regenerated cellulose materials from NMMO-solutions, *Progress in Polymer Science*, 26(9), 1473-1524.
- Fauziah M., Widiyastuti W., Balgis R., 2019, Production of cellulose aerogels from coir fibers via an alkali-urea method for sorption applications, *Cellulose*, 26, 9583-9598.
- Fauziah M., Widiyastuti W., Setyawan H., 2020, A hydrophobic cellulose aerogel from coir fibers waste for oil spill application, *IOP Conference Series Materials Science and Engineering*, 778, 012019.
- Goimil L., Braga M. E. M., Dias A. M. A., Gómez-Amoza J. L., Concheiro A., Alvarez-Lorenzo C., De Sousa H. C., García-González C. A., 2017, Supercritical processing of starch aerogels and aerogel-loaded poly(ϵ -caprolactone) scaffolds for sustained release of ketoprofen for bone regeneration, *Journal of CO₂ Utilization*, 18, 237-249.
- Kargarzadeh H., Mariano M., Gopakumar D., Ahmad I., Thomas S., Dufresne A., Huang J., Lin N., 2018, Advances in cellulose nanomaterials, *Cellulose*, 25, 2151-2189.
- Luo M., Wang M., Pang H., Zhang R., Huang J., Liang K., Chen P., Sun P., Kong B., 2021, Super-assembled highly compressible and flexible cellulose aerogels for methylene blue removal from water, *Chinese Chemical Letters*, 32(6), 2091-2096.
- Manzocco L., Mikkonen K. S., García-González C. A., 2021, Aerogels as porous structures for food applications: Smart ingredients and novel packaging materials, *Food Structure*, 28, 100188.
- Nguyen S. T., Feng J., Ng S. K., Wong J. P. W., Tan V. B. C., Duong H. M., 2014, Advanced thermal insulation and absorption properties of recycled cellulose aerogels, *Colloids and Surfaces A: Physicochemical and Engineering Aspects*, 445, 128-134.
- Oh S. Y., Yoo D. I., Shin Y., Kim H. C., Kim H. Y., Chung Y. S., Park W. H., Youk J. H., 2005, Crystalline structure analysis of cellulose treated with sodium hydroxide and carbon dioxide by means of X-ray diffraction and FTIR spectroscopy, *Carbohydrate Research*, 340(15), 2376-2391.
- Sarno M. C. C., 2019, Production of Nanocellulose from Waste Cellulose, *Chemical Engineering Transactions*, 73, 103-108.
- Swatoski R. P., Spear S. K., Holbrey J. D., Rogers R. D., 2002., Dissolution of Cellose with Ionic Liquids, *Journal of the American Chemical Society*, 124(18), 4974-4975.
- Wan K., Wang Z., He Y., Xia J., Zhou Z., Zhou J., Cen K., 2015, Experimental and modeling study of pyrolysis of coal, biomass and blended coal-biomass particles, *Fuel*, 139, 356-364.
- Yang T., Xiong X., Venkataraman M., Mishra R., Novák J., Militký J., 2019, Investigation on sound absorption properties of aerogel/polymer nonwovens, *Journal of the Textile Institute*, 110(2), 196-201.
- Yang X., Han F., Xu C., Jiang S., Huang L., Liu L., Xia, Z., 2017, Effects of preparation methods on the morphology and properties of nanocellulose (NC) extracted from corn husk, *Industrial Crops and Products*, 109, 241-247.